NANO LETTERS

Communication

Three-dimensional multifunctional magnetically-responsive liquid manipulator fabricated by femtosecond laser writing and soft transfer

Shaojun Jiang, Yanlei Hu, Hao Wu, Rui Li, Yiyuan Zhang, Chao Chen, Cheng Xue, Bing Xu, Wulin Zhu, Jiawen Li, Dong Wu, and Jiaru Chu

Nano Lett., **Just Accepted Manuscript** • DOI: 10.1021/acs.nanolett.0c02997 • Publication Date (Web): 11 Sep 2020

is published by the American Chemical Society. 1155 Sixteenth Street N.W., Washington, DC 20036

Three-dimensional multifunctional magnetically-responsive liquid manipulator fabricated by femtosecond laser writing and soft transfer

Shaojun Jiang, Yanlei Hu, Hao Wu, Rui Li, Yiyuan Zhang, Chao Chen, Cheng Xue, Bing Xu, Wulin Zhu, Jiawen Li, Dong Wu,* and Jiaru Chu*

CAS Key Laboratory of Mechanical Behavior and Design of Materials, Key Laboratory of Precision Scientific Instrumentation of Anhui Higher Education Institutes, Department of Precision Machinery and Precision Instrumentation, University of Science and Technology of China, Hefei 230027, China

E-mail: huyl@ustc.edu.cn; dongwu@ustc.edu.cn

Keywords: three-dimensional transport, liquid manipulation, magnetically-responsive structure, rapid propulsion, femtosecond laser

ABSTRACT: Nature-inspired magnetically-responsive intelligent topography surfaces have attracted considerable attention owing to their controllable droplet manipulation abilities. However, it's still challenging for magnetically-responsive surfaces to realize three-dimensional (3D) droplet/multi-droplet transport in both horizontal and vertical directions. Additionally, the droplet horizontal propulsion speed needs to be improved. In this work, a 3D droplet/multi-droplet transport strategy based on magnetically-responsive microplates array (MMA) actuated by spatially varying and periodic magnetic field is proposed. The modified superhydrophobic surface can transport droplets rapidly both in horizontal and vertical directions, and even realize against-gravity upslope propulsion. The rapid horizontal droplet propulsion (~58.6 mm/s) is ascribed to the abrupt inversion of the modified surface induced by

the specific magnetic field. Furthermore, the non-magnetically-responsive microplates (NMMs)/MMA composite surface is constructed to realize 3D multi-droplet manipulation. The implementations of MMA in manipulation of continuous fluids and liquid metal are further demonstrated, providing a valuable platform for microfluidic applications.

Organisms in nature use their unique surface structures to directionally and spontaneously transport droplets.[1-5] In practical applications, droplets manipulation is crucial for bioassays[6, 7] and chemical microreactions.[8, 9] Artificial passive droplet manipulation surfaces have been already prepared for energy-free droplets manipulation.[10-16] However, they are usually inefficient and irreversible. In contrast, intelligent topography surfaces can dynamically and reversibly change the surface topography in response to external stimuli such as mechanical forces,[17-19] pneumatic,[20] wet,[21, 22] magnetic field,[23-27] so as to realize the horizontal[23-26] or vertical[19-22, 27] droplets manipulation. Among them, the magnetically-responsive intelligent topography (MIT) surfaces have gained great expectations for active droplet manipulation due to their incomparable advantages including biocompatibility, instantaneous response and battery-free remote control.[23, 25]

Water droplet transportation including horizontal propulsion and vertical capture/release can be realized by the deformation of MIT surfaces with magnetically-induced bending structures.[23-30] The superhydrophobic micropillar/microwall can bend to generate asymmetric structures under the conventional magnetic fields. The contact angles at the opposite sides of the droplet become different on these asymmetric structures, resulting in surface tension forces imbalance-for driving the droplet.[23, 26, 28, 30] Another propulsion way is to form a local concave on the superhydrophobic micaopillar/microcilia array by magneto-induced clustering.[24, 25] Droplets can be propelled on-demand by driving force and potential energy difference caused by the cluster. Droplets can also be propelled by the collective beating of the magnetic micropillars by moving the conventional magnetic field.[29] In addition to the horizontal propulsion, vertical droplet capture/release can be realized by controlling the deformation of the magnetorheological micropillars with electromagnet to change their stiffness.[27] The contact between droplet and micropillars shifts from line contact to point contact with the increased stiffness. As a result, the droplet is released due to the decreased adhesion force. Despite diverse MIT surfaces have been widely used for controllable droplets transport, they can only realize single-direction transport (horizontal direction[23-26, 28-30] or vertical direction[27]). However, from the viewpoint of practical applications, multi-dimensional and rapid droplet transport is crucial for microchemistry and microfluidics. Some deficiencies still exist in the existing MIT surfaces: 1) It's still challenging for MIT surfaces to realize three-dimensional (3D) droplet/multi-droplet transport. Due to the low-adhesion superhydrophobic properties of the existing MIT surfaces, it's difficult to realize droplet against-gravity upslope propulsion, let alone vertical transport.[23-26, 28, 30] 2) The current MIT surfaces with magnetically-induced bending structures have limited droplet propulsion speed due to the dependence on gravity or surface tension imbalance (Table S1). 3) Limited by structural geometry (micropillar/microcilia array) and driving strategy (conventional magnetic fields induced bending), it's difficult for MIT surfaces to manipulate both discrete diverse droplets and continuous fluids. In this regard, seeking a 3D, fast, versatile liquid manipulation MIT surface is still an urgent need.

Herein, 3D droplet/multi-droplet transport is realized by the magnetically-responsive microplates array (MMA). Unlike other MIT surfaces for single-direction droplet transport,[23-30] the modified superhydrophobic MMA (SMMA) can not only propel droplets in the horizontal direction, but also capture/release droplets in the vertical direction due to the localized high adhesion on the top face of the microplates (Table S1). As a result of the periodic magnetic field induced high-frequency sequential abrupt inversion of SMMA, droplets can be propelled rapidly with an unprecedent speed up to ~58.6 mm/s. Droplets can also be propelled uphill along the inclined surface, which is a challenge for other low-adhesion superhydrophobic MIT surfaces.[23-26, 28, 30] In addition, the non-magnetically-responsive microplates (NMMs)/MMA composite surface is constructed for versatile 3D multi-droplet manipulations. The surface is further used to manipulate continuous fluids and to transport liquid metal, which has potential applications in reconfigurable antenna and soft robotics.[31-33]

The MMA is fabricated by femtosecond laser writing and soft transfer technology (Figure 1a).[34-37] The surface is then modified by a superhydrophobic spray to enhance the hydrophobicity and reduce the surface adhesion (termed as SMMA, variation of sliding angles is shown in Figure S1). Figure 1b shows the tilted-view scanning electron microscopy (SEM) image of the untreated surface. After modification, the surface is covered by superhydrophobic materials consisting of ~40 nm nanoparticles (Figure 1c).[38, 39] Most of the top area is covered by superhydrophobic materials, but a small portion remains exposed and has high adhesion to water droplet (Figure 1d, Figure S2). However, the sidewall is completely covered (Figure 1e). The SMMA enables 3D droplets transport due to the high adhesion in locally exposed areas at the top of the microplates. Droplet can be propelled rapidly in horizontal direction due to the inertia and adhesion force (Figure 1f). Two-dimensional droplet transport can also be realized (Figure S3). Moreover, droplet can be captured vertically by the surface due to the localized high adhesion of the end face, and released by magnetically-controlled bending (Figure 1g).

Microplates can bend along the direction of the magnetic field owing to the internal carbonyl iron particles chains.[40, 41] Magnets array with the same magnetic poles facing together has a special spatially varying and periodic magnetic field (Figure S4) with periodic polarity change regions (dashed black frames in Figure 2a). The microplate can gradually bend with the approach of the magnets array and reaches its maximum bending degree when it is located above the polarity change region. As the magnets array moves, the direction of the magnetic field to which the microplate is exposed suddenly changes. So the microplate can be abruptly inversed. (Figure 2a) Under the periodic magnetic field, periodic abrupt inversion of the microplates can be realized. The magnetic flux density at different positions of the magnets array is shown in Figure 2b and Figure S5 (~0 mT-~681 mT). The bending property of the microplate (height of ~940 μm, width of ~93 μm, length of ~2.39 mm, the same hereinafter) is systematically characterized under the magnetic field (Figure 2b, Figure S6). At both ends of the polarity change region where the magnetic flux density is ~0 mT, the bending angles (α) are the largest, reaching ~28.2°±2.5° and ~-32.5°±5.3° respectively.

The horizontal droplet transport can be realized by the sequential abrupt inversion of microplates (Figure 2c), which can be subdivided into six steps: (ⅰ) The droplet first sits on the microplates 2&3, and (ⅱ) gradually moves to the left with the bending of the microplates as the magnets array approaches the bottom of SMMA. (ⅲ) The microplate 1 is abruptly inversed when the polarity change region passes through (in less than 8 ms with the magnets speed of ~285 mm/s) and contacts with the droplet. (ⅳ) The microplate 2 is also abruptly inversed as the polarity change region passes through. During this process, the droplet remains in contact with the top of the three microplates due to the inertia and adhesion force. (ⅴ) The microplate 3 is abruptly inversed with the top separating from the droplet. Due to the inertia and the adhesion force, the droplet remains on the top of the microplates 1&2. At this time, the droplet completes the transfer from microplates 2&3 to 1&2. (ⅵ) As the magnets array moves away, the droplet is driven to the left as the microplates gradually regain verticality. Optical images of the transport process are shown in Figure 2d. The droplet is moved forward by the surface with distances of d_1 and d_2 in step Ⅰ and step Ⅲ, respectively. However, it remains in place in step Ⅱ due to the inertia and adhesion force and only the microplates undergo a sequential bending inversion. The distance that the droplet moves once is proportional to the microplate interval (Figure S7, Movie S1).

Droplet can be transported continuously with the rapid movement of the magnets array. (Movie S2) The droplet transport speed ($S_{droplet}$) is proportional to the magnets array moving speed (S) and microplate interval (I), which can be expressed by (elaborated in detail in the Supporting Information)

$$S_{droplet} \approx \frac{N \times I \times S}{L_1 - N \times I}$$

where N refers to the numbers of polarity change regions on the magnets array (N=8). And L_1 is the distance between the first and the last polarity change regions (~174.4 mm).

Droplet transport speed increases linearly with magnets moving speed and microplate interval (Figure 2e, g). The volume (V) has neglectable impact (<0.71 mm/s) on droplet speed with an average transport speed of ~23.05 mm/s (Figure 2f, 2-5 μL). The 6 μL droplet is more likely to stick to the top of three microplates simultaneously during transport due to the large diameter and gravity. Additional adhesion resistance is created, resulting in reduced transport speed (~15.31 mm/s, Figure S8). The experimental results are in good agreement with the theoretical analysis (Figure 2e-h). The droplet transport distance is linearly correlated with time (Figure 2h). In-situ observation of droplet transport is shown in Figure S8-S10. In comparison, untreated MMA is also used for horizontal droplet transport. However, droplet gets stuck between microplates due to the entire high adhesion of the surface (Figure S11, Movie S3). Compared with other magnetically-induced bending surfaces, the sequential abrupt inversion of SMMA induced by periodic magnetic field enables interval-by-interval droplet transport. The fast-moving magnetic field induces high-frequency sequential inversion of the surface (fast-oscillating). Due to the localized high adhesion on the top of the microplates, droplet can be rapidly transported on the fast-oscillating surface. Each rapid oscillation of microplates drives the droplet to transport a distance of I. The maximum achievable speed is ~58.6 mm/s (S~1231.95 mm/s, I=993 μm, V=4 μL, Table S1). However, it's difficult to transport droplets by the surface with conventional magnetic fields (not periodic, Figure S12, Movie S4). The superhydrophobicity and fast droplet transport capability of the SMMA maintain long-term stability even under external mechanical/physical perturbations (Figure S13).

Droplet can move back and forth with the reciprocating motion of the magnets array (Figure 3a, b). A droplet moves quickly to the right under the left-moving magnets array in ~0.3 s, and moves back to the initial position in ~0.9 s (Movie S5). Unlike other homogeneous magnetically-responsive structures for single-droplet manipulation, the non-magnetically-responsive microplates (NMMs)/MMA composite surface is constructed (Figure S14) for multi-droplet manipulation (Figure 3c-e). The red droplet on the superhydrophobic modified composite surface is transported rapidly (~23.34 mm/s) to the left induced by the fast-moving magnetic field, and merges with the blue droplet in ~0.31 s (Movie S6). The composite surface can be applied as a miniature reactor for rapid microchemical reactions. The copper sulfate ($CuSO_4$) droplet can be rapidly transported (~20.5 mm/s) and react with the sodium hydroxide (NaOH) droplet to form copper hydroxide ($Cu(OH)_2$) precipitates (~0.28 s, Figure 3e, Movie S7).

The SMMA can even realize against-gravity climbing propulsion of droplet on an inclined surface by the periodic magnetic field induced high-frequency sequential abrupt inversion. The localized high adhesion on the top of the microplates and the droplet inertia allow droplet to transport on the inclined surface, which is a challenge for other low-adhesion superhydrophobic MIT surfaces (Table S1). A droplet can climb up (~20 mm/s) an inclined surface (~5.4°) with a parallel moving magnetic field (Figure 3f, Movie S8).

The SMMA can transport droplet in both horizontal and vertical directions. Water droplet can be vertically captured by the surface because the exposed areas on the top of the microplates (Figure S2) have strong adhesion. When the magnetic field (generated by two jointed magnets, 40×40×20 mm, ~0.34 T at the junction) is applied above the surface, the droplet can be released by the structural bending (Figure 4a, Movie S9). The bending angle versus magnetic flux density is shown in Figure S15. The droplet adhesion states are displayed in Figure 4b. The left column shows the initial state where the resultant force of adhesion forces (F_L and F_R) is equal to the droplet gravity (G, $F_L+F_R=G$) The three-phase contact lines equally distribute on the top of two microplates (Figure S16). As the magnets get closer, the microplates begin to bend (the middle column of Figure 4b), the vertical force components can be described as follows

$$F_{L\perp}\cos\alpha_1+F_{L/\!/}\sin\alpha_1+F_{R\perp}\cos\alpha_1+F_{R/\!/}\sin\alpha_1=G \quad (1)$$

where $F_{L\perp}$ and $F_{L/\!/}$ are the adhesion forces perpendicular to and parallel to the end face of the left microplate, respectively. And $F_{R\perp}$ and $F_{R/\!/}$ are the corresponding forces on the right microplate. To simplify the calculation, the microplate is regarded as a rigid body with the bending angle of α. The bending angles of the two microplates are approximately equal at the beginning of the bend (α_1). The right column shows the droplet gradually slides down from the end face of the left microplate. The non-uniformly distributed magnetic field causes the bending angle of the left microplate (α_2) to be slightly larger than that of the right microplate (α_3), causing droplet to gradually slide down the left microplate which is closer to the magnets. The inclination of the end face increases gradually with the bending angle, which further induces droplet sliding. The contact area between the droplet and the microplate decreases as the droplet slides down. Therefore, the three-phase contact lines become shorter and the adhesion force decreases (Figure S16).[27, 42] The resultant force of adhesion force in the vertical direction can be evaluated by the Equation (2)

$$F'_{L\perp}\cos\alpha_2+F'_{L/\!/}\sin\alpha_2+F'_{R\perp}\cos\alpha_3+F'_{R/\!/}\sin\alpha_3<G \quad (2)$$

where $\alpha_2>\alpha_3>\alpha_1$. With the increase of the bending angle, the droplet gradually detaches from the left microplate and finally drips.

The release angle (α) gradually decreases with the increase of droplet volume from 2 μL to 5 μL (I=593 μm, Figure 4c). The vertical manipulation capabilities of untreated MMA and SMMA are investigated (Figure 4d, Figure S17). Droplets can be captured/released vertically by the surfaces (region ⅱ). However, large droplets are difficult to be captured (region ⅰ). And small droplets are difficult to be released even when the microplates bend to the maximum angle (region ⅲ). Vertical manipulation of small droplets (2 μL) to large droplets (10 μL) can be realized by the surfaces with different treatments (superhydrophobic treatment and no treatment).

Droplets targeted release and merging can be realized by using SMMA (Figure 4e). Water droplet 1 is captured and horizontally transported. It can be released by magnetically-controlled bending and merge with droplet 2 (Movie S10). Moreover, the superhydrophobic modified NMMs/MMA composite surface can realize vertical multi-droplet capture and selective release, which is a challenge for homogeneous magnetorheological micropillars[27] (Figure 4f, Movie

S11). Two droplets are captured by the composite surface. The droplet on the SMMA can be released by the structural deformation while the other droplet is still captured by the NMMs.

Rapid mixing of different fluids is crucial for the microfluidic systems.[43, 44] Magnetism-based micromixer has advantages of remote control and instantaneous response.[44, 45] On-demand control of continuous fluids can also be realized by MMA under the periodic magnetic field. Two different dyed ethanol solutions are pumped into the MMA-integrated microfluidic channel and effectively mixed by the MMA micromixer by rapid oscillation (Figure 5a, Movie S12).

The MMA is further applied to transport liquid metals (LMs). LMs are unique metallic materials that maintain a liquid phase at room temperature with superior thermal/electrical conductivities and favorable fluidity.[31, 46, 47] Here, a new strategy to directionally propel LM by using the MMA is proposed. LM droplet can be directionally propelled by the sequential abrupt inversion of the surface without coating/mixing with ferromagnetic particles (Figure 5b, c). So the intrinsic properties of LM will not be affected.[31, 48, 49] The surface (after hydrophilic treatment) is placed in an aqueous environment. Water can form an interfacial slip layer to prevent the sticky oxide layer of LM from adhering to the surface.[33] As shown in Figure 5c, (ⅰ) LM droplet is first dropped onto the surface. (ⅱ) It moves to the left slightly along with the microplates as the magnets array approaches. (ⅲ) LM droplet is propelled to the right due to the abrupt inversion of the microplates when the first polarity change region (indicated by the black arrow) passes through. (ⅳ) As the magnets array moves further, the microplates are inversed sequentially. (ⅴ-ⅷ) When the second polarity change region (indicated by the brown arrow) passes, the LM droplet is propelled to the right again. The motion curves are shown in Figure 5d. The LM droplet first moves to the left slightly when the first polarity change region approaches (distance reduction) and is propelled to the right as the polarity change region reaches below it (two curves intersect). When the second polarity change region approaches, the previous process is repeated.

In summary, 3D droplet/multi-droplet transport is achieved by the magnetically-responsive manipulator under the spatially varying and periodic magnetic field. Based on the periodic magnetic field induced high-frequency sequential abrupt inversion of microplates, the droplet horizontal propulsion speed reaches ~58.6 mm/s, which is faster than that of other magnetically-induced bending surfaces. Multiple 3D droplet transport modes such as horizontal propulsion, against-gravity climbing propulsion, vertical positioning-capture/targeted-release can be realized. In addition, the composite surface is constructed for 3D multi-droplet manipulation such as rapid microscopic positioning merging, microchemical reaction and multi-droplet parallel-capture/selective-release. The microplates array can further apply as a micromixer to remotely mix continuous fluids. Furthermore, the coating-free and chemical reaction-free liquid metal directional propulsion is demonstrated. The as-prepared magnetically-responsive manipulator owns versatile liquid manipulation functions, providing a valuable platform for 3D multifunctional droplet manipulation in the fields of microchemistry and microfluidics.

Materials and Methods

Fabrication of MMA: First, a series of regular rectangular holes are fabricated on the shape memory polystyrene (SMP) polymer sheet by femtosecond laser direct writing. And then the SMP sheet shrinks completely by heating in an oven at 130 °C for 9 min. After a double-sided tape sticking on the one end of the shrunk SMP sheet, the liquid polydimethylsiloxane (PDMS) doped with carbonyl iron powder is casted into the SMP sheet and then degassed. In order to assemble iron particles into chains to obtain a strong magnetic response, a neodymium-iron-boron (NdFeB) permanent magnet (40 × 40 × 20 mm) is placed below the sample for ~5 s. After that, the sample is cured on the heating plate (100 ℃, 0.5 h). The MMA can be acquired after the sample (polystyrene mould) is successively treated in toluene solution for 1 h, in deionize water for 10 min and in ethanol for another 10 min under the ultrasonic environment.

Preparation of carbonyl iron powder doped PDMS: Liquid polydimethylsiloxane prepolymer (Sylgard 184, Dow Corning), crosslinker and carbonyl iron powder (3-5 μm, ≥99.5% purity, Nangong Rui Teng Alloy Material Co., Ltd.) were thoroughly mixed by hand in a weight ratio of 10: 3.5: 1. After that the mixture was degassed in a vacuum chamber for ~30 min to remove the bubbles completely. After degassed, the carbonyl iron powder doped PDMS can be acquired.

Femtosecond Laser Fabrication: The regular rectangular holes were constructed on the SMP sheet by femtosecond laser direct writing. The laser beam (central wavelength of 800 nm, repetition rate of 1 kHz, pulse width of 104 fs) from a regenerative amplified Ti:sapphire femtosecond laser system (Legend Elite-1K-HE, Coherent, USA) was guided onto the SMP surface through a galvanometric system (SCANLAB, Germany). The laser beam was focused on the SMP sheet by the telecentric f-theta lens (focused length of 63 mm). The laser power, scanning speed and scanning repetition were set at 250 mW, 25 mm s^{-1}, and 50 circles, respectively.

Materials: The SMP polymers with average thickness of ~150 μm were obtained from Hebei Bean Pod Network Technology Co., Ltd.. The shrinkage ratio is about 60%. The glass transition temperature of the SMP polymer is ~107 ℃. Double-sided tape was provided by Kapton, TED PELLA Inc., USA. Two different types of NdFeB magnets (rectangular magnet with parameters of 40 × 40 × 20 mm, magnets array with diameter of 25 mm and total length of 204 mm) were purchased from Shanghai Ze He Mechanical & electrical co., Ltd.. In the demoulding process, the sample was treated in toluene (C_7H_8, ≥ 99.5% purity, 0.865 g cm^{-3}density) solution under the ultrasonic environment for 1 h to dissolve the polystyrene mold. And then the acquired MMA surface was further treated in the deionize water and ethanol (C_2H_6O > 99.7% purity, 0.798 g cm^{-3} density) solution under the ultrasonic environment for 10 min, respectively. After ultrasonic treatment, the swelling of PDMS caused by toluene can be eliminated. The commercial superhydrophobic spray (Glaco Mirror Coat Zero, Soft 99 Ltd, Japan) and hydrophilic spray (Quick Clear, Soft 99 Ltd, Japan) were used to further enhance the hydrophobicity and hydrophily of MMA surface, respectively. In this work, EGaIn (75% Ga, 25% In) LM was used for directionally propulsion.

Characterization: The different microstructures of MMA and SMMA were characterized by using a secondary electron SEM (ZEISS EVO18). The optical images were taken by a high-speed charge-coupled device camera (120 fps, MER-030-120UM/UC, China Daheng Group, Inc.). Each reported droplet speed was an average of at least eight independent measurements. The liquids mixing process was recorded by a digital camera. A digital Gauss meter (HM-100, Huaming instrument Co., Ltd., China) was used to measure the magnetic flux density and the COMSOL Multiphysics 5.3a software was used to simulate the magnetic field.

ASSOCIATED CONTENT

Supporting Information

The following files are available free of charge.

Movie S1: Detailed water droplet horizontal transport process on the SMMA surface (AVI)

Movie S2: Continuous and rapid horizontal transport of the water droplet on the SMMA surface (AVI)

Movie S3: Water droplet gets stuck on the untreated MMA surface (AVI)

Movie S4: Water droplet can't be transported on the SMMA surface under the excitation of conventional magnetic fields (AVI)

Movie S5: Reciprocating motion of the water droplet on the SMMA surface (AVI)

Movie S6: Directional transport and rapid microscopic positioning merging of water droplets on the superhydrophobic modified NMMs/MMA composite surface (AVI)

Movie S7: Rapid microchemical reactions on the superhydrophobic modified NMMs/MMA composite surface (AVI)

Movie S8: Against-gravity climbing transport of the water droplet on the SMMA surface (AVI)

Movie S9: Vertical capture and release of the water droplet by the inverted SMMA surface (AVI)

Movie S10: Vertical capture, horizontal transport and on-demand release of water droplets (AVI)

Movie S11: Vertical capture and selective release of multi-droplet by the superhydrophobic modified NMMs/MMA composite surface (AVI)

Movie S12: Remote control of fluids mixing in a microfluidic chip by the untreated MMA surface (AVI)

Variation of sliding angles of MMA and SMMA; detailed SEM images of the top of microplates; two-dimensional water droplet transport; simulation of magnetic field; the measured magnetic flux density of magnets array; bending angle of the microplate corresponding to different positions of the magnets array; distance curve of water droplet transport; in-situ observation of water droplets transport process on the SMMA surface under different parameters (magnets array moving speed, droplet volume and microplate interval); motion process of the water droplet on the untreated MMA surface; motion states of water droplets on SMMA actuated by conventional magnetic fields; water contact angle of SMMA under ultrasonic and high-temperature environments; schematic illustration of the fabrication procedure of the NMMs/MMA composite surface; magnetic response bending properties of the microplate; adhesion states of SMMA to water droplet and the distribution of three-phase contact lines at different bending angles; three different vertical manipulation states of water droplets; detailed analysis of water droplet transport speed; comparison of droplet transport performance of MIT surfaces in existing studies (PDF)

AUTHOR INFORMATION

Corresponding Authors

*E-mail: huyl@ustc.edu.cn

*E-mail: dongwu@ustc.edu.cn

Author Contributions

S.J., Y.H. and D.W. designed the experiment. C.X., H.W., and W.Z. fabricated samples. Y.Z., and R.L. performed the experiments. C.C. and B.X. conducted the simulations. S.J. analyzed the data and prepared the manuscript. J.L., D.W., Y.H. and J.C. reviewed and revised the manuscript.

Notes

The authors declare no competing financial interest.

Acknowledgements

This work was supported by the National Natural Science Foundation of China (Nos. 51875544, 51675503, 51805509), the Fundamental Research Funds for the Central Universities (WK2090000013, WK2090090021, WK2090090024, WK2090090025, WK6030000131), Youth Innovation Promotion Association CAS (2017495), Foundation of Equipment Development Department (6220914010901). Thanks for the USTC Center for Micro and Nanoscale Research and Fabrication.

References

(1) Ju, J.; Bai, H.; Zheng, Y.; Zhao, T.; Fang, R.; Jiang, L. A multi-structural and multi-functional integrated fog collection system in cactus. *Nat. Commun.* **2012,** 3, 1247.
(2) Malik, F. T.; Clement, R. M.; Gethin, D. T.; Krawszik, W.; Parker, A. R. Nature's moisture harvesters: a comparative review. *Bioinspiration Biomimetics* **2014,** 9, 031002.
(3) Chen, H.; Ran, T.; Gan, Y.; Zhou, J.; Zhang, Y.; Zhang, L.; Zhang, D.; Jiang, L. Ultrafast water harvesting and transport in hierarchical microchannels. *Nat. Mater.* **2018,** 17, 935-942.
(4) Chen, H.; Zhang, P.; Zhang, L.; Liu, H.; Jiang, Y.; Zhang, D.; Han, Z.; Jiang, L.

Continuous directional water transport on the peristome surface of Nepenthes alata. *Nature* **2016,** 532, 85-89.
(5) Wang, Q.; Yao, X.; Liu, H.; Quere, D.; Jiang, L. Self-removal of condensed water on the legs of water striders. *Proc. Natl. Acad. Sci. U. S. A.* **2015,** 112, 9247-9252.
(6) Zhang, Y.; Wang, T. H. Full-range magnetic manipulation of droplets via surface energy traps enables complex bioassays. *Adv. Mater.* **2013,** 25, 2903-2908.
(7) Zhang, Y.; Park, S.; Liu, K.; Tsuan, J.; Yang, S.; Wang, T. H. A surface topography assisted droplet manipulation platform for biomarker detection and pathogen identification. *Lab Chip* **2011,** 11, 398-406.
(8) Yang, Y.; Li, X.; Zheng, X.; Chen, Z.; Zhou, Q.; Chen, Y. 3D-Printed Biomimetic Super-Hydrophobic Structure for Microdroplet Manipulation and Oil/Water Separation. *Adv. Mater.* **2018,** 30, 1704912.
(9) Tan, Y.; Hu, B.; Chu, Z.; Wu, W. Bioinspired Superhydrophobic Papillae with Tunable Adhesive Force and Ultralarge Liquid Capacity for Microdroplet Manipulation. *Adv. Funct. Mater.* **2019,** 29, 1900266.
(10) Yu, C.; Zhang, L.; Ru, Y.; Li, N.; Li, C.; Gao, C.; Dong, Z.; Jiang, L. Drop Cargo Transfer via Unidirectional Lubricant Spreading on Peristome-Mimetic Surface. *ACS Nano* **2018,** 12, 11307-11315.
(11) Bai, H.; Wang, L.; Ju, J.; Sun, R.; Zheng, Y.; Jiang, L. Efficient water collection on integrative bioinspired surfaces with star-shaped wettability patterns. *Adv. Mater.* **2014,** 26, 5025-5030.
(12) Park, K. C.; Kim, P.; Grinthal, A.; He, N.; Fox, D.; Weaver, J. C.; Aizenberg, J. Condensation on slippery asymmetric bumps. *Nature* **2016,** 531, 78-82.
(13) Wang, M.; Liu, Q.; Zhang, H.; Wang, C.; Wang, L.; Xiang, B.; Fan, Y.; Guo, C. F.; Ruan, S. Laser Direct Writing of Tree-Shaped Hierarchical Cones on a Superhydrophobic Film for High-Efficiency Water Collection. *ACS Appl. Mater. Interfaces* **2017,** 9, 29248-29254.
(14) Geng, H.; Bai, H.; Fan, Y.; Wang, S.; Ba, T.; Yu, C.; Cao, M.; Jiang, L. Unidirectional water delivery on a superhydrophilic surface with two-dimensional asymmetrical wettability barriers. *Mater. Horiz.* **2018,** 5, 303-308.
(15) Li, J.; Zhou, X.; Li, J.; Che, L.; Yao, J.; McHale, G.; Chaudhury, M. K.; Wang, Z. Topological liquid diode. *Sci. Adv.* **2017,** 3, eaao3530.
(16) Li, J.; Li, J.; Sun, J.; Feng, S.; Wang, Z. Biological and Engineered Topological Droplet Rectifiers. *Adv. Mater.* **2019,** 31, e1806501.
(17) Wu, D.; Wu, S. Z.; Chen, Q. D.; Zhang, Y. L.; Yao, J.; Yao, X.; Niu, L. G.; Wang, J. N.; Jiang, L.; Sun, H. B. Curvature-driven reversible in situ switching between pinned and roll-down superhydrophobic States for water droplet transportation. *Adv. Mater.* **2011,** 23, 545-549.
(18) Yao, X.; Hu, Y.; Grinthal, A.; Wong, T. S.; Mahadevan, L.; Aizenberg, J. Adaptive fluid-infused porous films with tunable transparency and wettability. *Nat. Mater.* **2013,** 12, 529-534.
(19) Tang, X.; Zhu, P.; Tian, Y.; Zhou, X.; Kong, T.; Wang, L. Mechano-regulated surface for manipulating liquid droplets. *Nat. Commun.* **2017,** 8, 14831.
(20) Wang, J.-N.; Liu, Y.-Q.; Zhang, Y.-L.; Feng, J.; Sun, H.-B. Pneumatic smart surfaces with rapidly switchable dominant and latent superhydrophobicity. *NPG Asia Mater.* **2018,** 10, e470.

(21) Wang, Y.; Lai, H.; Cheng, Z.; Zhang, H.; Liu, Y.; Jiang, L. Smart Superhydrophobic Shape Memory Adhesive Surface toward Selective Capture/Release of Microdroplets. *ACS Appl. Mater. Interfaces* **2019**, 11, 10988.

(22) Wang, Y.; Lai, H.; Cheng, Z.; Zhang, H.; Zhang, E.; Lv, T.; Liu, Y.; Jiang, L. Gecko toe pads inspired in situ switchable superhydrophobic shape memory adhesive film. *Nanoscale* **2019,** 11, 8984-8993.

(23) Lin, Y.; Hu, Z.; Zhang, M.; Xu, T.; Feng, S.; Jiang, L.; Zheng, Y. Magnetically Induced Low Adhesive Direction of Nano/Micropillar Arrays for Microdroplet Transport. *Adv. Funct. Mater.* **2018**, 28, 1800163.

(24) Ben, S.; Zhou, T.; Ma, H.; Yao, J.; Ning, Y.; Tian, D.; Liu, K.; Jiang, L. Multifunctional Magnetocontrollable Superwettable-Microcilia Surface for Directional Droplet Manipulation. *Adv. Sci.* **2019**, 1900834.

(25) Kim, J. H.; Kang, S. M.; Lee, B. J.; Ko, H.; Bae, W. G.; Suh, K. Y.; Kwak, M. K.; Jeong, H. E. Remote Manipulation of Droplets on a Flexible Magnetically Responsive Film. *Sci. Rep.* **2015,** 5, 17843.

(26) Yang, Z.; Park, J. K.; Kim, S. Magnetically Responsive Elastomer-Silicon Hybrid Surfaces for Fluid and Light Manipulation. *Small* **2018,** 14, 1702839.

(27) Yang, C.; Wu, L.; Li, G. Magnetically Responsive Superhydrophobic Surface: In Situ Reversible Switching of Water Droplet Wettability and Adhesion for Droplet Manipulation. *ACS Appl. Mater. Interfaces* **2018,** 10, 20150-20158.

(28) Wang, L.; Zhang, M.; Shi, W.; Hou, Y.; Liu, C.; Feng, S.; Guo, Z.; Zheng, Y. Dynamic Magnetic Responsive Wall Array with Droplet Shedding-off Properties. *Sci. Rep.* **2015,** 5, 11209.

(29) Al-Azawi, A.; Cenev, Z.; Tupasela, T.; Peng, B.; Ikkala, O.; Zhou, Q.; Jokinen, V.; Franssila, S.; Ras, R. H. A. Tunable and Magnetic Thiol-ene Micropillar Arrays. *Macromol. Rapid Commun.* **2020,** 41, e1900522.

(30) Wang, Z.; Wang, K.; Liang, D.; Yan, L.; Ni, K.; Huang, H.; Li, B.; Guo, Z.; Wang, J.; Ma, X.; Tang, X.; Chen, L. Q. Hybrid Magnetic Micropillar Arrays for Programmable Actuation. *Adv. Mater.* **2020**, e2001879.

(31) Wu, J.; Tang, S. Y.; Fang, T.; Li, W.; Li, X.; Zhang, S. A Wheeled Robot Driven by a Liquid-Metal Droplet. *Adv. Mater.* **2018,** 30, e1805039.

(32) Yu, Y.; Miyako, E. Recent Advances in Liquid Metal Manipulation toward Soft Robotics and Biotechnologies. *Chem. - Eur. J.* **2018,** 24, 9456-9462.

(33) Khan, M. R.; Trlica, C.; So, J. H.; Valeri, M.; Dickey, M. D. Influence of water on the interfacial behavior of gallium liquid metal alloys. *ACS Appl. Mater. Interfaces* **2014,** 6, 22467-22473.

(34) Jiang, S.; Hu, Y.; Wu, H.; Zhang, Y.; Zhang, Y.; Wang, Y.; Zhang, Y.; Zhu, W.; Li, J.; Wu, D.; Chu, J. Multifunctional Janus Microplates Arrays Actuated by Magnetic Fields for Water/Light Switches and Bio-Inspired Assimilatory Coloration. *Adv. Mater.* **2019,** 31, e1807507.

(35) Li, Z. Z.; Wang, L.; Fan, H.; Yu, Y. H.; Sun, H. B.; Juodkazis, S.; Chen, Q. D. O-FIB: far-field-induced near-field breakdown for direct nanowriting in an atmospheric environment.

Light: Sci. Appl. **2020,** 9, 41.
(36) Malinauskas, M.; Zukauskas, A.; Hasegawa, S.; Hayasaki, Y.; Mizeikis, V.; Buividas, R.; Juodkazis, S. Ultrafast laser processing of materials: from science to industry. *Light: Sci. Appl.* **2016,** 5, e16133.
(37) Sugioka, K.; Cheng, Y. Ultrafast lasers—reliable tools for advanced materials processing. *Light: Sci. Appl.* **2014,** 3, e149-e149.
(38) Vakarelski, I. U.; Patankar, N. A.; Marston, J. O.; Chan, D. Y.; Thoroddsen, S. T. Stabilization of Leidenfrost vapour layer by textured superhydrophobic surfaces. *Nature* **2012,** 489, 274-277.
(39) Jetly, A.; Vakarelski, I. U.; Thoroddsen, S. T. Drag crisis moderation by thin air layers sustained on superhydrophobic spheres falling in water. *Soft Matter* **2018,** 14, 1608-1613.
(40) Schmauch, M. M.; Mishra, S. R.; Evans, B. A.; Velev, O. D.; Tracy, J. B. Chained Iron Microparticles for Directionally Controlled Actuation of Soft Robots. *ACS Appl. Mater. Interfaces* **2017,** 9, 11895-11901.
(41) Kim, J.; Chung, S. E.; Choi, S. E.; Lee, H.; Kim, J.; Kwon, S. Programming magnetic anisotropy in polymeric microactuators. *Nat. Mater.* **2011,** 10, 747-752.
(42) Cao, M.; Jin, X.; Peng, Y.; Yu, C.; Li, K.; Liu, K.; Jiang, L. Unidirectional Wetting Properties on Multi-Bioinspired Magnetocontrollable Slippery Microcilia. *Adv. Mater.* **2017,** 29, 1606869.
(43) Lim, T. W.; Son, Y.; Jeong, Y. J.; Yang, D. Y.; Kong, H. J.; Lee, K. S.; Kim, D. P. Three-dimensionally crossing manifold micro-mixer for fast mixing in a short channel length. *Lab Chip* **2011,** 11, 100-103.
(44) Zhou, B.; Xu, W.; Syed, A. A.; Chau, Y.; Chen, L.; Chew, B.; Yassine, O.; Wu, X.; Gao, Y.; Zhang, J.; Xiao, X.; Kosel, J.; Zhang, X. X.; Yao, Z.; Wen, W. Design and fabrication of magnetically functionalized flexible micropillar arrays for rapid and controllable microfluidic mixing. *Lab Chip* **2015,** 15, 2125-2132.
(45) Chen, C. Y.; Chen, C. Y.; Lin, C. Y.; Hu, Y. T. Magnetically actuated artificial cilia for optimum mixing performance in microfluidics. *Lab Chip* **2013,** 13, 2834-2839.
(46) Ma, B.; Xu, C.; Chi, J.; Chen, J.; Zhao, C.; Liu, H. A Versatile Approach for Direct Patterning of Liquid Metal Using Magnetic Field. *Adv. Funct. Mater.* **2019,** 29, 1901370.
(47) Yun, G.; Tang, S. Y.; Sun, S.; Yuan, D.; Zhao, Q.; Deng, L.; Yan, S.; Du, H.; Dickey, M. D.; Li, W. Liquid metal-filled magnetorheological elastomer with positive piezoconductivity. *Nat. Commun.* **2019,** 10, 1300.
(48) Shu, J.; Tang, S. Y.; Feng, Z.; Li, W.; Li, X.; Zhang, S. Unconventional locomotion of liquid metal droplets driven by magnetic fields. *Soft Matter* **2018,** 14, 7113-7118.
(49) Carle, F.; Bai, K.; Casara, J.; Vanderlick, K.; Brown, E. Development of magnetic liquid metal suspensions for magnetohydrodynamics. *Phys. Rev. Fluids* **2017,** 2, 013301.

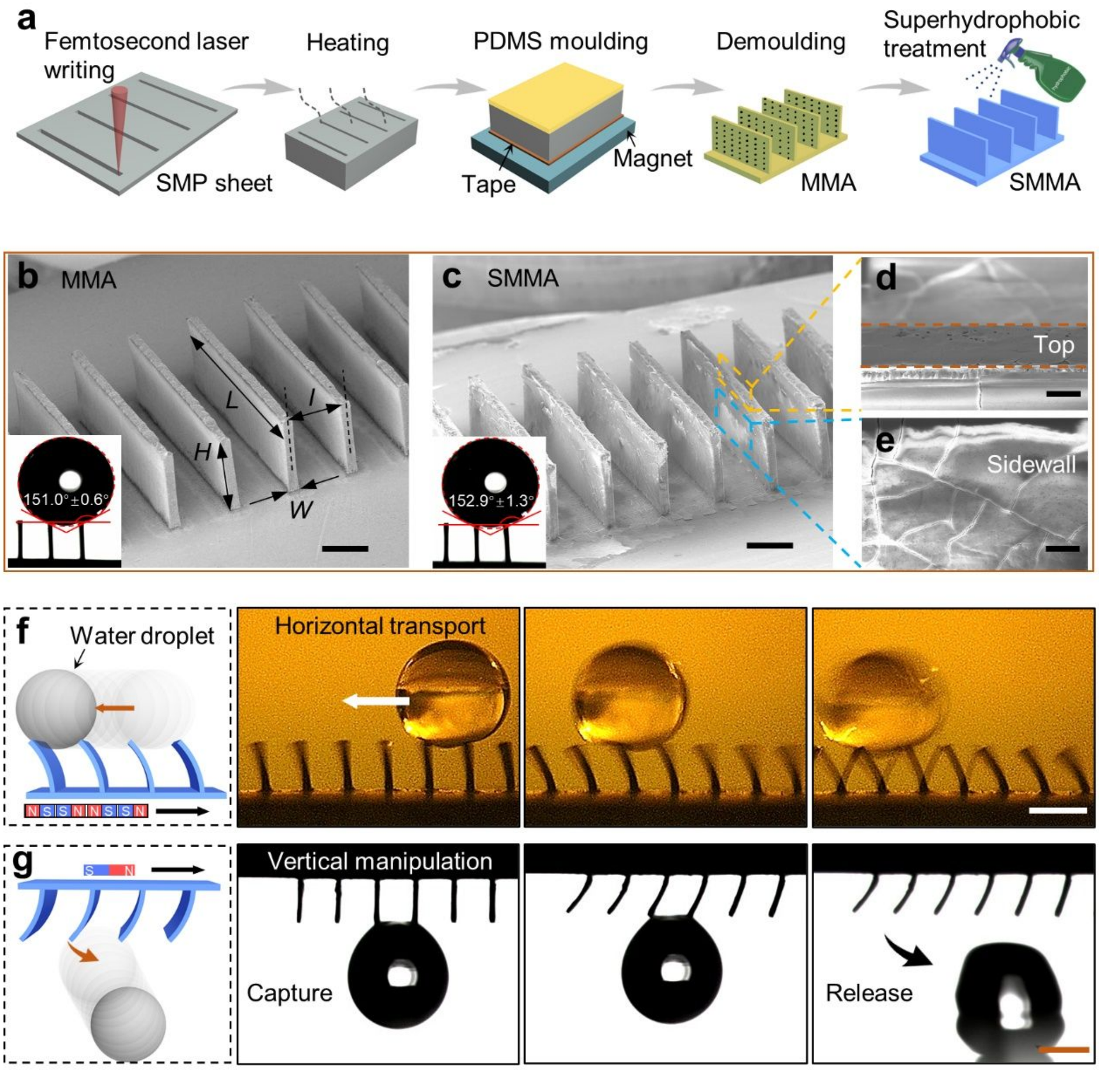

Figure 1. Fabrication procedure of the SMMA and its distinct 3D droplet manipulation. (a) Schematic illustration of the fabrication procedure of MMA and SMMA. (b) SEM image of the MMA with height (*H*) of ~940 μm, width (*W*) of ~93 μm, length (*L*) of ~2.39 mm and interval (*I*) of ~689 μm. The inset shows the water contact angle of the MMA surface. Scale bar: 500 μm. (c) SEM image of the SMMA. There's a layer of superhydrophobic material consisting of ~40 nm silica nanoparticles on the whole surface. The inset shows that water contact angle is slightly increased (from initial 151.0° ± 0.6° to 152.9° ± 1.3°) after treatment. Scale bar: 500 μm. (d, e) Magnified SEM images of the SMMA. Both the (d) top surface and the (e) sidewall are covered by the superhydrophobic material. However, there are still some exposed areas on the top surface, which have a higher adhesion to water droplet than the superhydrophobic areas. This localized high adhesion is critical in 3D droplet transport. Scale bars: 50 μm. (f, g) Schematic illustration and optical images of the horizontal propulsion and vertical capture/release of water droplet, respectively. (f) Water droplet can be propelled rapidly in the horizontal direction by SMMA under the excitation of a moving periodic magnetic field due to the inertia and adhesion force. (g) Water droplet can be captured vertically

by the inverted SMMA due to the localized high adhesion of the end face of the microplates. It can be released by the structural deformation of inverted SMMA. Scale bars: 1 mm.

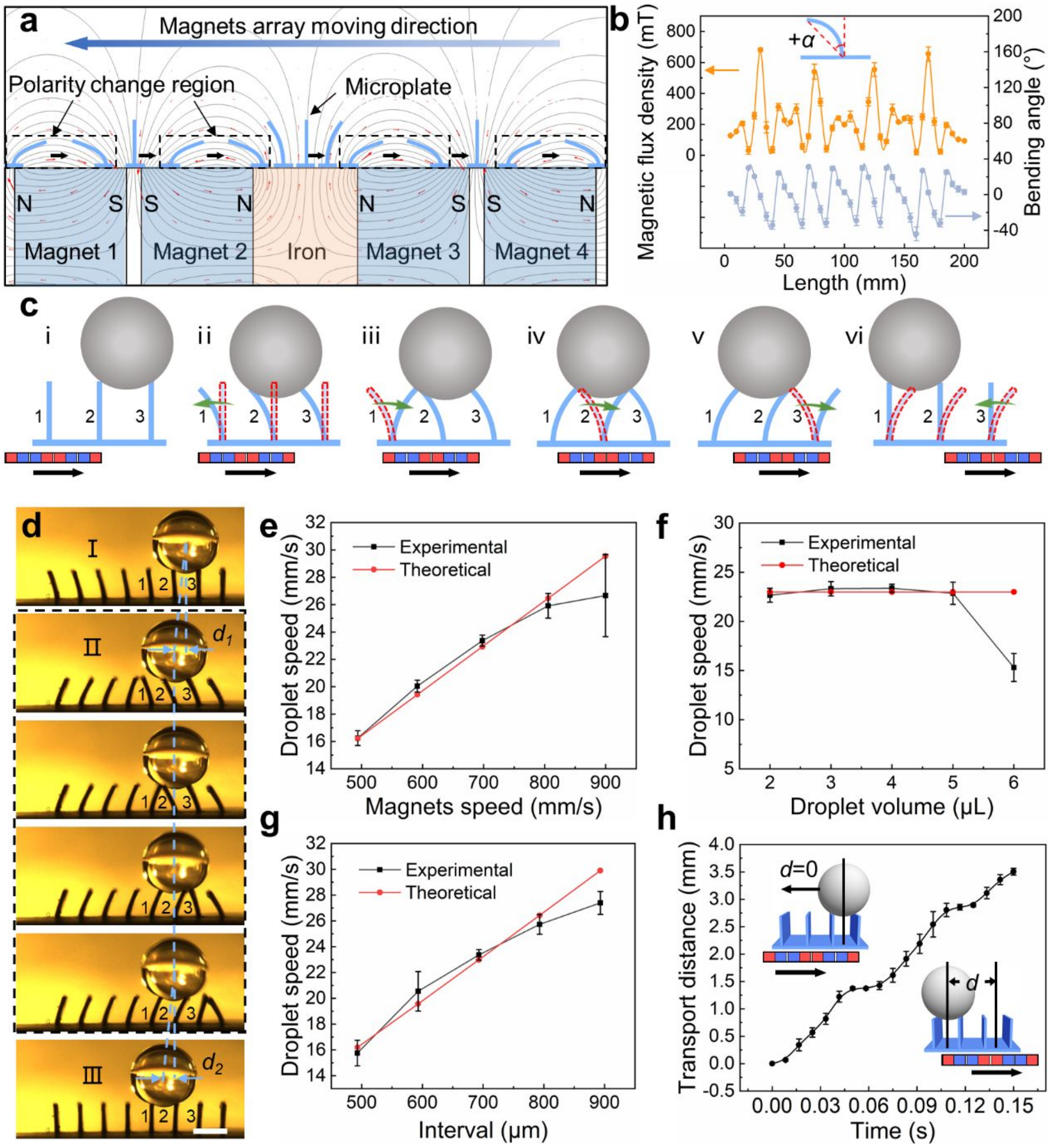

Figure 2. The magnetic response characteristics of SMMA based on a spatially varying and periodic magnetic field and the mechanism of water droplet transport. (a) Simulation of magnetic field and the schematic diagram of microplate bending. Microplate bends to align with the magnetic field (the microplate is fixed and the magnets array moves to the left). The abrupt inversion of bending angle occurs in the polarity change region (indicated by the dashed black frames). (b) Magnetic flux density and bending angles at different positions of the magnets array. The inset shows that the left bending angle is defined as positive. The signs of the angles indicate that the bending directions are opposite. (c) Schematic diagram of the horizontal transport of a water droplet on SMMA surface under the excitation of the periodic magnetic field. The red dashed lines represent the previous states of the microplates. (d) Optical

images of the water droplet (4 μL) transport process on the SMMA surface. Scale bar: 1 mm. (e-g) Experimental results of the droplet transport speed versus (e) magnets speed (V=4 μL, I=693 μm), (f) droplet volume (S=700 mm/s, I=693 μm) and (g) interval of microplates (V=4 μL, S=700 mm/s). (h) Water droplet transport distance versus time (V=4 μL, S=700 mm/s, I=693 μm). The insets are schematic drawings of the transport distance "d" of the water droplet.

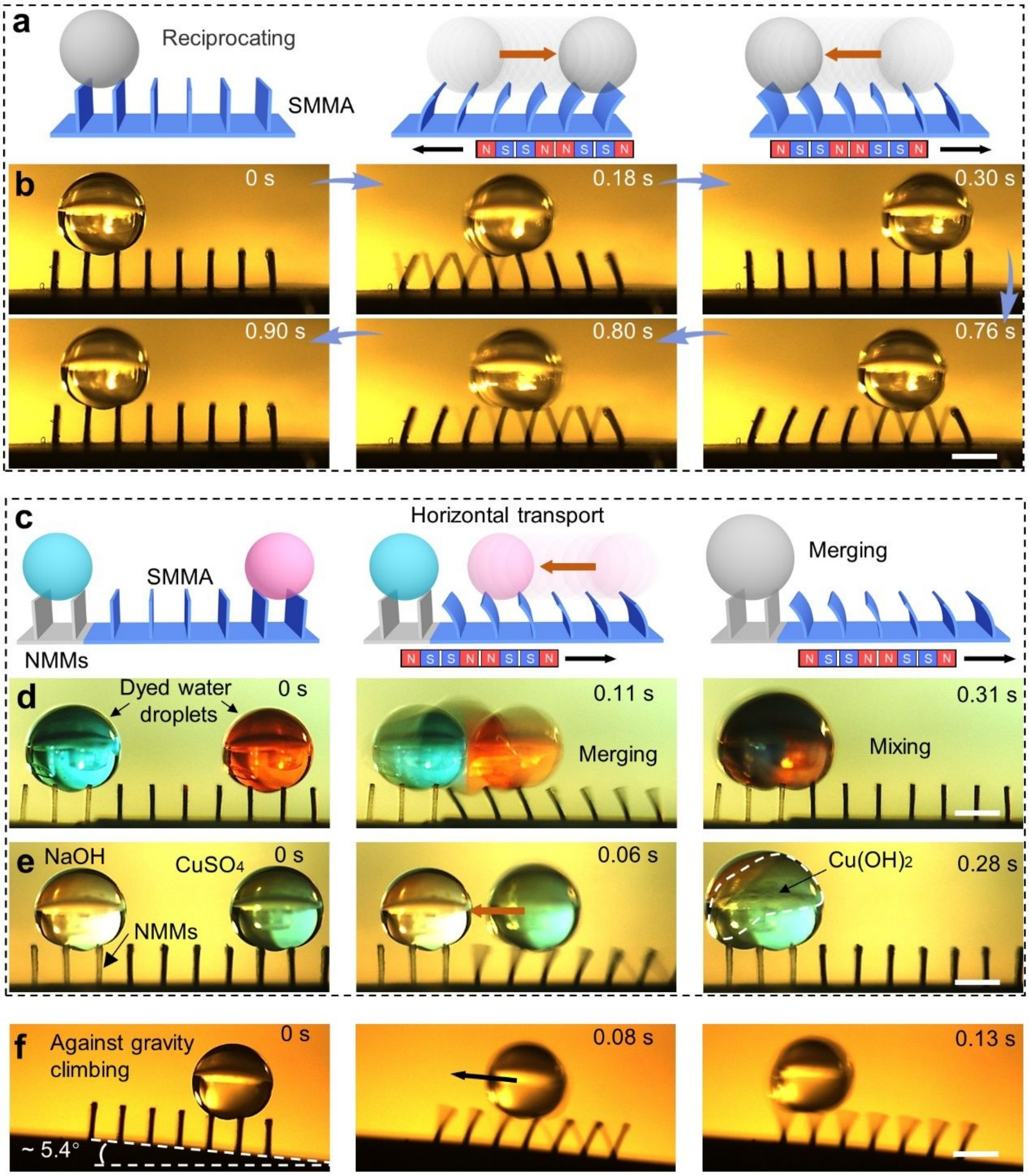

Figure 3. Horizontal manipulation and against-gravity climbing propulsion of water droplets on the SMMA surface. (a, b) Schematic diagram and optical images of droplet moving back and forth on the SMMA under the reciprocating periodic magnetic field, respectively (V=4 μL, I=693 μm). (c, d) Schematic illustration and detailed working process of directional propulsion, merging and mixing of water droplets on the superhydrophobic treated NMMs/MMA composite surface, respectively (V~5 μL, I=793 μm, S=700 mm/s). (e) A simple

chemical reaction based on the rapid droplet horizontal propulsion and microscopic positioning merging. The $CuSO_4$ droplet is quickly transported to the left and reacts with NaOH droplet at a fixed point (V~5 μL, I=793 μm, S=700 mm/s) to form blue $Cu(OH)_2$ precipitates (dashed white line). (f) Optical images of a water droplet (V~3 μL) climbing up an inclined SMMA surface with an inclination angle of ~5.4 °. All scale bars: 1 mm.

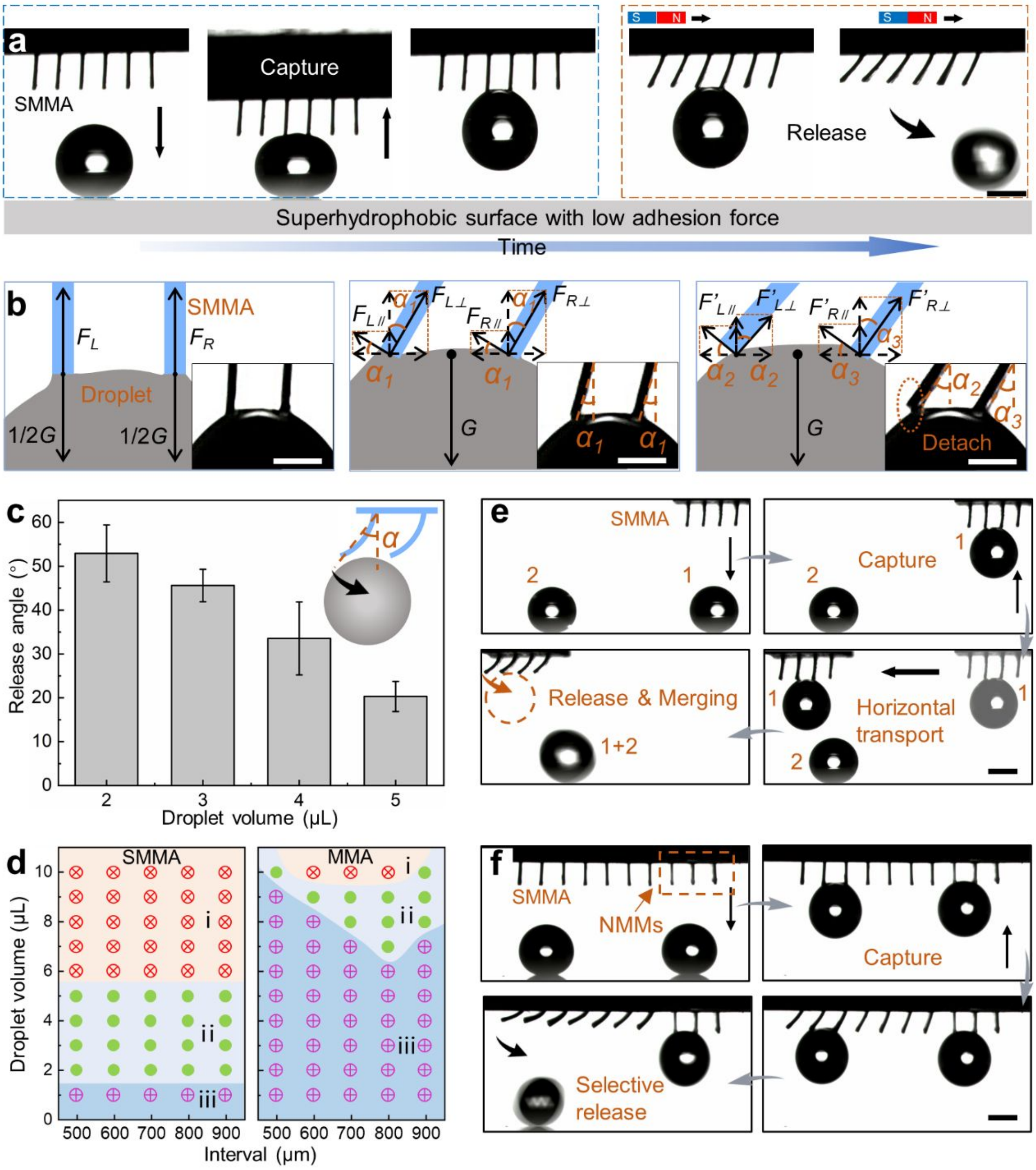

Figure 4. Vertical droplet manipulation mechanism and versatile applications based on the vertical droplet manipulation. (a) Optical images of the vertical water droplet manipulation. Water droplet on the low adhesion superhydrophobic surface can be captured by the inverted SMMA due to the localized high adhesion of the end face of the microplates. Under the excitation of a magnetic field, the droplet can be released due to the bending of the microplates (V=4 μL, I=593 μm). Scale bar: 1 mm. (b) Analysis of the mechanism of vertical

droplet manipulation. Scale bares are 500 μm. (c) The quantitative relationship between water droplet volume and release angle (α). The α gradually decreases from ~52.92°±6.5° to ~20.30°±3.4° with the increase of volume from 2 μL to 5 μL. The inset is the schematic drawing of the release angle (α). (d) The phase diagram revealing vertical manipulation capabilities of untreated MMA and SMMA with different intervals. The green dots in region ⅱ represent that the water droplet can be successfully captured and released by the structures (‘capture-release’ state). Pink cross symbols in region ⅲ indicate that water droplet can be captured but cannot be released (‘release-failed’ state). And the red cross symbols in region ⅰ indicate that water droplet cannot be captured (‘capture-failed’ state). (e) Vertical capture, horizontal transport and on-demand release of water droplets (V=3 μL, I=593 μm). (f) Optical images of parallel vertical capture and selective release of multi-droplet by the superhydrophobic treated NMMs/MMA composite surface. Scale bars of (e, f) are 1 mm.

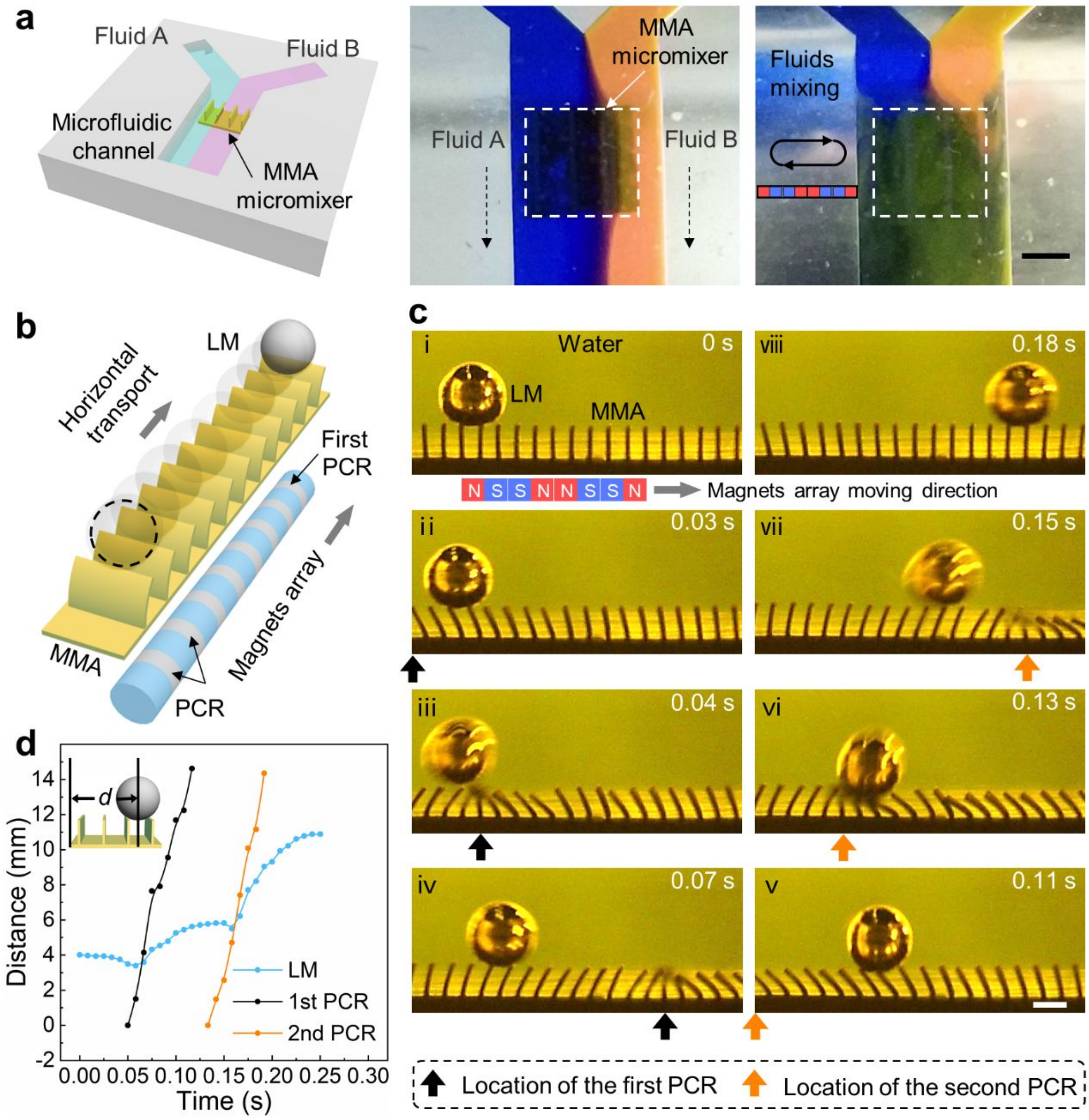

Figure 5. Manipulation of continuous fluids and liquid metal based on MMA surface. (a) Schematic illustration and photos of remote controllable fluids mixing in a microfluidic chip. Two different dyed ethanol solutions are effectively mixed by the MMA micromixer (l=893 μm) under the reciprocating motion of the periodic magnetic field. (b, c) Schematic illustration and optical images of the directional propulsion of LM droplet (~1 μL) by the sequential abrupt inversion of MMA (l=493 μm) under the periodic magnetic field (water environment), respectively. The polarity change region (PCR) is indicated by black arrow. (d) The motion curves of LM and PCR. The inset is the schematic drawing of the transport distance "*d*" of the LM droplet. The leftmost side of MMA is defined as d=0. All scale bars: 1 mm.

For Table of Contents Only

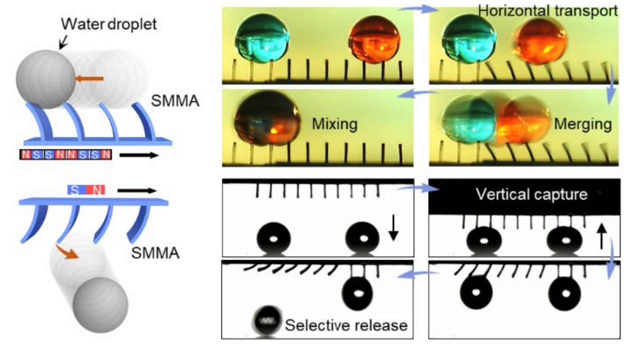

A three-dimensional multifunctional liquid manipulator based on magnetically-responsive microplates array enables water droplet transport in both horizontal and vertical directions. This manipulator is actuated by periodic magnetic fields, leading to an exceptional droplet propulsion speed. It can be used for diverse manipulations of discrete droplet, continuous fluids and liquid metal.